

# Hyperoxia results in increased aerobic metabolism following acute brain injury

Arnab Ghosh<sup>1,\*</sup>, David Highton<sup>1,\*</sup>, Christina Kolyva<sup>2</sup>, Ilias Tachtsidis<sup>2</sup>, Clare E Elwell<sup>2</sup> and Martin Smith<sup>1,2,3</sup>

Journal of Cerebral Blood Flow & Metabolism

0(00) 1–11

© Author(s) 2016

Reprints and permissions:

sagepub.co.uk/journalsPermissions.nav

DOI: 10.1177/0271678X16679171

jcbfm.sagepub.com



## Abstract

Acute brain injury is associated with depressed aerobic metabolism. Below a critical mitochondrial  $pO_2$  cytochrome c oxidase, the terminal electron acceptor in the mitochondrial respiratory chain, fails to sustain oxidative phosphorylation. After acute brain injury, this ischaemic threshold might be shifted into apparently normal levels of tissue oxygenation. We investigated the oxygen dependency of aerobic metabolism in 16 acutely brain-injured patients using a 120-min normobaric hyperoxia challenge in the acute phase (24–72 h) post-injury and multimodal neuromonitoring, including transcranial Doppler ultrasound-measured cerebral blood flow velocity, cerebral microdialysis-derived lactate-pyruvate ratio (LPR), brain tissue  $pO_2$  ( $p_{br}O_2$ ), and tissue oxygenation index and cytochrome c oxidase oxidation state (oxCCO) measured using broadband spectroscopy. Increased inspired oxygen resulted in increased  $p_{br}O_2$  [ $\Delta p_{br}O_2$  30.9 mmHg  $p < 0.001$ ], reduced LPR [ $\Delta LPR$   $-3.07$   $p = 0.015$ ], and increased cytochrome c oxidase (CCO) oxidation ( $\Delta [oxCCO] + 0.32 \mu M$   $p < 0.001$ ) which persisted on return-to-baseline ( $\Delta [oxCCO] + 0.22 \mu M$ ,  $p < 0.01$ ), accompanied by a 7.5% increase in estimated cerebral metabolic rate for oxygen ( $p = 0.038$ ). Our results are consistent with an improvement in cellular redox state, suggesting oxygen-limited metabolism above recognised ischaemic  $p_{br}O_2$  thresholds. Diffusion limitation or mitochondrial inhibition might explain these findings. Further investigation is warranted to establish optimal oxygenation to sustain aerobic metabolism after acute brain injury.

## Keywords

Brain ischaemia, energy metabolism, mitochondria, near infrared spectroscopy, neurocritical care

Received 2 June 2016; Revised 2 September 2016; Accepted 17 October 2016

## Introduction

The brain relies on aerobic metabolism to meet its substantial energy needs and, in health, various mechanisms ensure that oxygen (and metabolic substrate) supply is balanced to meet metabolic demand. This balance is often disturbed after acute brain injury in which cerebral hypoxia–ischaemia is a key injury mechanism associated with poor outcome, irrespective of brain injury type.<sup>1–3</sup> Specific neuroprotective therapies have failed to translate into clinical benefit<sup>4,5</sup> and treatment of severe acute brain injury therefore focuses on avoiding or minimising secondary cerebral hypoxia–ischaemia and consequent mitochondrial energy failure by maintaining cerebral oxygen delivery at a level that is sufficient to meet metabolic demand.<sup>6,7</sup> Debate continues whether depressed aerobic metabolism, which is common following acute brain injury, predominantly

reflects oxygen deprivation or a non-ischaemic metabolic crisis.<sup>8,9</sup>

Mitochondria exist and function normally in a near anoxic environment, facilitating a diffusion gradient for oxygen transport from the microvasculature, and

<sup>1</sup>Neurocritical Care, University College London Hospitals, National Hospital for Neurology & Neurosurgery, London, UK

<sup>2</sup>Department of Medical Physics and Biomedical Engineering, University College London, London, UK

<sup>3</sup>University College London Hospitals National Institute for Health Research Biomedical Research Centre, London, UK

\*These authors contributed equally to this work.

### Corresponding author:

David Highton, Neurocritical Care, University College London Hospitals, National Hospital for Neurology & Neurosurgery, Queen Square, London WC1N 3BG, UK.  
Email: d.highton@ucl.ac.uk

offering protection from oxidant damage. Cytochrome *c* oxidase (CCO), the terminal electron acceptor in the mitochondrial respiratory chain, is responsible for reducing oxygen to water. Its low Michaelis–Menton constant ( $K_m$ ) for oxygen means that oxidative phosphorylation may continue unimpeded in isolated mitochondria with a  $pO_2$  less than 1 mmHg.<sup>10</sup> Below a critical ischaemic threshold, CCO is reduced and, importantly, oxygen then becomes a rate limiting substrate decreasing oxidative phosphorylation.<sup>11,12</sup>

In health, changes of brain tissue  $pO_2$  within the physiological range are not believed to influence cerebral oxygen consumption<sup>13</sup> but, following acute brain injury, a range of disturbances to oxygen transport and its utilisation may complicate the relationship between  $pO_2$  and metabolism. Classical ischaemia describes a situation of insufficient oxygen delivery, and therefore of maximal extraction of oxygen from haemoglobin, and is characterized by a combination of large oxygen extraction fraction (OEF) measured by positron emission tomography (PET), cerebral oligoemia, and falling cerebral metabolic rate for oxygen (CMRO<sub>2</sub>).<sup>14</sup> While prevalent early after acute brain injury, this picture is less common beyond the immediate period of injury after stroke and traumatic brain injury (TBI).<sup>15</sup> Metabolic dysfunction has been identified in the presence of apparently acceptable tissue oxygenation, where both diffusion limited oxygen transport and mitochondrial dysfunction have been implicated as alternative forms of restriction to oxidative metabolism in the presence of a normal interstitial tissue  $pO_2$  or OEF.<sup>16</sup>

Multimodal neuromonitoring with brain tissue  $pO_2$  ( $p_{br}O_2$ ) and cerebral microdialysis-derived lactate:pyruvate ratio (LPR) have enabled investigation of the relationship between oxygen delivery, cerebral tissue oxygenation, and cellular redox status in vivo following TBI,<sup>16</sup> aneurysmal subarachnoid haemorrhage (SAH),<sup>17</sup> and intracerebral haemorrhage (ICH).<sup>18,19</sup> Clinical therapy protocols guided by changes in  $p_{br}O_2$  seek to maintain oxygen delivery and availability above a ‘critical’  $pO_2$  threshold for anaerobic metabolism.<sup>20</sup> Although overt ischaemia and anaerobic metabolism has typically been described when  $p_{br}O_2$  falls below 10 mmHg, normobaric hyperoxia and hyperbaric hyperoxia may improve LPR and CMRO<sub>2</sub> after TBI in the presence of  $p_{br}O_2$  values that are within or above the normal physiological range.<sup>21–23</sup> Vespa et al.<sup>16</sup> demonstrated metabolic dysfunction without classical ischaemia after TBI based on observation of elevated LPR and PET-derived OEF > 0.75. Others have described a similar picture of metabolic dysfunction ‘without hypoxia’ in SAH and ICH.<sup>17</sup> However, it is difficult to entirely rule out hypoxia as a cause of such observations because of the absence of a subcellular marker of oxygenation in these studies. Diffusion

limitation or an altered mitochondrial ischaemic threshold could equally explain these findings. While CCO oxidation status reflects the activity of the respiratory chain, it is also dependent on metabolic substrate supply, ATP, oxygen, and mediators which modify the  $K_m$  for oxygen such as nitric oxide.<sup>24</sup> Understanding the changes in CCO oxidation status may therefore be a useful adjunct for the in-vivo investigation of diffusion limitation and mitochondrial dysfunction after acute brain injury.

We have developed an in-house optical technique, incorporating hybrid spatially resolved broadband and frequency domain near infrared spectroscopy (NIRS), optimised for the measurement of the oxidation state of CCO [oxCCO] in adult brain-injured patients.<sup>25</sup> Spatially resolved cerebral tissue oxygen saturation, also called the tissue oxygenation index (TOI), in association with concentrations of oxyhaemoglobin ([HbO<sub>2</sub>]), deoxyhaemoglobin ([HHb]) and [oxCCO] may be used to investigate oxygenation of both the microvasculature and mitochondria.<sup>12</sup> A comprehensive multimodal neuromonitoring array, including  $p_{br}O_2$ , microdialysis, transcranial Doppler-measured cerebral blood flow velocity and NIRS therefore covers the entire oxygen cascade from the microvasculature (TOI, HbO<sub>2</sub>, HHb) through the tissue interstitium ( $p_{br}O_2$ ) to the mitochondria ([oxCCO]), and has potential to predict cellular redox status (microdialysis LPR, [oxCCO]) and CMRO<sub>2</sub> changes estimated using NIRS and transcranial Doppler,<sup>26</sup> and might therefore differentiate between diffusion limited oxygen transport and mitochondrial dysfunction.

The aim of this study was to investigate the oxygen dependence of mitochondrial metabolism in vivo following acute brain injury. We hypothesised that normobaric hyperoxia-induced increases in cerebral oxygen availability would lead to an increase in CCO oxidation and reduction in microdialysate LPR, suggesting oxygen-limited mitochondrial oxidative metabolism at baseline.

## Materials and methods

### Study participants and protocol

After approval by the Research Ethics Committee of the National Hospital for Neurology and Neurosurgery and Institute of Neurology (04/Q0512/67) and representative consent, recordings were carried out in 16 sedated, mechanically ventilated acute brain injury patients requiring invasive neuromonitoring to guide clinical management on the neurocritical care unit. This was performed in accordance with the Declaration of Helsinki. Inclusion criteria also included baseline inspired fraction of oxygen (FiO<sub>2</sub>)

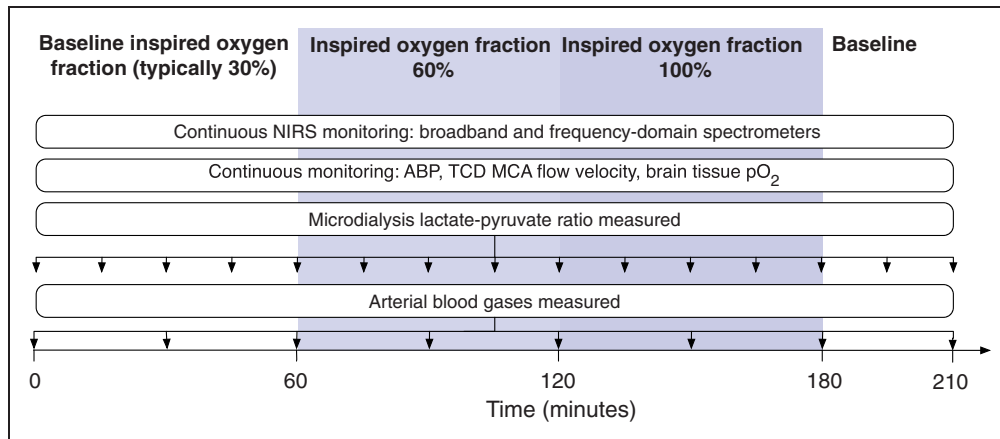


**Figure 1.** Normobaric hyperoxia protocol and measured variables.

less than 0.5. The patients were subject to a normobaric hyperoxia protocol which consisted of a 60-min epoch of baseline recording followed by two 60-min epochs in which  $\text{FiO}_2$  was increased first to 0.6 and then to 1.0, and a final 30-min epoch during which  $\text{FiO}_2$  was returned to baseline values (Figure 1).

### Monitored parameters

Systemic physiological monitoring included invasive arterial blood pressure (ABP) and pulse oximetry ( $\text{SpO}_2$ ) measured continuously, and measurement of arterial blood gases (ABGs), including carbon dioxide and oxygen partial pressures ( $\text{paCO}_2$  and  $\text{paO}_2$ , respectively). Middle cerebral artery blood flow velocity ( $V_{\text{mca}}$ ) was measured using transcranial Doppler ultrasonography (DWL Doppler Box, Compumedics, Singen, Germany). Invasive cerebral monitoring comprised  $\text{p}_{\text{br}}\text{O}_2$  (Licox, Integra Neurosciences, Plainsboro, USA) and measurement of LPR by cerebral microdialysis (M Dialysis AB, Stockholm, Sweden), with catheters implanted via a cranial access device (Technicam, Newton Abbot UK or Licox IP2, Integra Neurosciences) or surgically at time of craniotomy. In accordance with consensus guidelines, catheters were placed in peri-lesional tissue in patients with focal TBI or ICH, in the right frontal lobe in patients with diffuse TBI, or tissue thought to be at risk of ischaemia from vasospasm in patients with aneurysmal SAH.<sup>27</sup> All non-invasive cerebral monitoring was conducted ipsilateral to the invasive monitoring.

### NIRS instrumentation and processing

The NIRS apparatus used in this study has been described in detail elsewhere.<sup>28</sup> In brief it comprises two components – a multidistance broadband spectrometer and a multidistance frequency domain spectrometer.

Chromophore concentration was derived from the broadband spectroscopy component that incorporates a 50 W halogen light source and lens-based spectrograph based on a charge-coupled device camera (PIXIS 512f, Princeton instruments) using the UCLn algorithm.<sup>29</sup> Measurements were made simultaneously at four source-detector separations (20/25/30/35 mm). The broadband spectrometer-derived concentrations of  $\text{HbO}_2$ , HHb and oxCCO from the 35 mm separation are reported here as we have previously shown that this source-detector separation has the highest brain-specificity, particularly for the measurement of oxCCO.<sup>25</sup> The frequency domain component of the system utilises an OxyPlexTS device (ISS Inc., Champaign, IL, USA) modified with diodes emitting light at four wavelengths (690, 750, 790 and 850 nm), and was used to derive the absolute optical absorption and reduced scattering coefficients ( $\mu_a$  and  $\mu_s$ , respectively) as previously described,<sup>28</sup> and derivation of the differential pathlength factor using the diffusion approximation.<sup>30</sup> In this study, we report  $\mu_s$  recorded at 790 nm. An individual differential pathlength factor was calculated for each patient, based on the  $\mu_a$  and  $\mu_s$  measured by the frequency domain spectrometer during the initial minute of recording of the baseline epoch. The TOI – defined as  $[\text{HbO}_2]/([\text{HbO}_2]+[\text{HHb}])$  – was calculated using spatially resolved spectroscopy.<sup>31</sup> The 740 nm–900 nm wavelength range was used to resolve for  $\text{HbO}_2$ , HHb, and water, and TOI calculated using individual scattering values measured with the frequency domain system.<sup>25</sup>

NIRS data analysis was performed in Matlab 2010b (Mathworks, Natick, MA). Differential concentrations of  $\text{HbO}_2$ , HHb and oxCCO ( $\Delta[\text{HbO}_2]$ ,  $\Delta[\text{HHb}]$  and  $\Delta[\text{oxCCO}]$ , respectively) were calculated using the UCLn algorithm.<sup>28–30</sup> Changes in total haemoglobin concentration ( $\Delta[\text{HbT}]$ ) were calculated as  $\Delta[\text{HbO}_2] + \Delta[\text{HHb}]$  and in haemoglobin difference concentration ( $\Delta[\text{HbDiff}]$ ) as  $\Delta[\text{HbO}_2] - \Delta[\text{HHb}]$ .

## Data processing

After manual identification and linear interpolation to remove NIRS signal artefacts, mean values for each monitored variable were calculated for individual epochs for each patient. The continuously monitored systemic and cerebral variables (including NIRS) were synchronized, and a mean value from a period comprising  $\geq 50\%$  of the epoch which was free from noise was used for analysis. For intermittently sampled variables (i.e. ABGs and microdialysate LPR), the mean of all readings per epoch (minimum two per epoch) was used as the summary variable for that epoch.

Relative estimated changes in  $\text{CMRO}_2$  ( $\text{rCMRO}_2$ ) were estimated for the return-to-baseline epoch compared to the baseline epoch using the NIRS Fick equation (equation (1)) described by Roche-Labarbe et al.<sup>32</sup>

$$\text{rCMRO}_2 = \frac{\text{Vmca}}{\text{Vmca}_0} \cdot \left( \frac{\text{SpO}_2 - \text{TOI}}{\text{SpO}_{20} - \text{TOI}_0} \right) \quad (1)$$

## Statistical analysis

We used GLIMMPSE, a validated model for power calculation in linear mixed models,<sup>33</sup> to conduct a sample size calculation. Assuming an  $\Delta[\text{oxCCO}]$  standard deviation of  $0.2 \mu\text{M}$  in each epoch, a total of 16 patients are required to provide a power of 90% in detecting  $\Delta[\text{oxCCO}]$  changes of  $+0.1$ ,  $+0.2$  and  $+0.05 \mu\text{M}$  during the  $\text{FiO}_2=0.6$ ,  $\text{FiO}_2=1.0$  and return-to-baseline epochs.

Statistical analyses were carried out in R.<sup>34</sup> Parameters of interest were analysed using a mixed effects model,<sup>35</sup> modelling individual subjects as random and epochs as fixed effects. The significance of the fixed epoch effect for each variable (i.e. the probability that the variable was the same across all four epochs) was then estimated using the Likelihood Ratio Test, comparing the mixed effects model to a null model comprising only random effects. In variables with an epoch effect probability of  $<0.05$ , subsequent pairwise comparison between baseline and subsequent  $\text{FiO}_2$  epochs (0.6 and 1.0 and return-to-baseline), was performed using Bonferroni-corrected Wilcoxon signed-rank tests. The Hodges–Lehman estimate was used to calculate the (pseudo)median and per-epoch 95% confidence intervals. Relative changes in  $\text{CMRO}_2$  were similarly treated, but no Bonferroni correction was applied since only the baseline and return-to-baseline epochs were compared. All data are expressed as (pseudo)median (95% confidence interval) unless otherwise stated. A Spearman correlation was used to assess the relationship between baseline  $\text{pbrO}_2$  and LPR and the  $\Delta\text{LPR}$  response to normobaric hyperoxia. Statistical significance was inferred at  $p < 0.05$ .

## Results

The full study protocol was completed in all 16 patients. Patient characteristics are shown in Table 1. Technical failure resulted in the loss of ABP and  $\text{pbrO}_2$  recordings for one patient but this patient was included in all analyses, excluding these parameters. Baseline levels for the physiological variables are shown in Table 2, the epoch effect for each variable in Table 3, and changes in measured variables in Table 4 and Figure 2.

Normobaric hyperoxia was associated with statistically significant increases in  $\text{paO}_2$ ,  $\text{SpO}_2$  and  $\text{pbrO}_2$ , but there was no change in  $\text{paCO}_2$  during the study. While a significant overall epoch effect for  $\text{Vmca}$

**Table 1.** Demographic data.

Age (years)	46.5 (39.3–51.5)
Sex	6 male, 10 female
Primary diagnosis	TBI 7 SAH 8 ICH 1
Time to study (hours post injury)	36 (25.5–45)
Admission GCS	7 (4–9)

Note: Data expressed as median with IQR.

GCS: Glasgow coma score; ICH: intracerebral haemorrhage; SAH: subarachnoid haemorrhage; TBI: traumatic brain injury.

**Table 2.** Physiological & optical variables at baseline.

Variable	Baseline value (IQR)
$\text{FiO}_2$	0.325 (0.28–0.35)
$\text{paO}_2$ (kPa)	15.7 (12.5–18.0)
$\text{paCO}_2$ (kPa)	4.85 (4.65–4.97)
$\text{SpO}_2$ (%)	99 (98–99)
MAP (mmHg)	91.5 (83.2–96.8)
$\text{Vmca}$ ( $\text{cm}\cdot\text{s}^{-1}$ )	52.1 (48.7–71.8)
$\text{pbrO}_2$ (mmHg)	17.5 (12.0–24.4)
Microdialysate LPR	25.3 (23.5–33.5)
TOI (%)	72.8 (65.5–77.0)
DPF	9.33 (6.75–10.8)
$\mu\text{s}$ ( $\text{cm}^{-1}$ )	11.1 (6.76–12.4)

DPF: differential pathlength factor;  $\text{FiO}_2$ : inspired oxygen fraction; IQR: inter-quartile range; MAP: mean arterial blood pressure; LPR: lactate:pyruvate ratio;  $\text{paO}_2$ : arterial  $\text{pO}_2$ ;  $\text{paCO}_2$ : arterial  $\text{pCO}_2$ ;  $\text{pbrO}_2$ : brain tissue  $\text{pO}_2$ ; TOI: tissue oxygenation index;  $\text{SpO}_2$ : arterial oxygen saturation;  $\mu\text{s}$ : optical reduced scattering coefficient;  $\text{Vmca}$ : middle cerebral artery blood flow velocity.

**Table 3.** Epoch effects from likelihood ratio test.

Variable	Chi-squared	<i>p</i>
paO <sub>2</sub>	171	<0.001
pCO <sub>2</sub>	5.63	0.131
SpO <sub>2</sub>	64.8	<0.001
LPR	9.28	0.026
pbrO <sub>2</sub>	44.6	<0.001
Vmca	8.31	0.04
HbDiff	27.0	<0.001
HbT	4.5	0.21
oxCCO	15.1	0.002
TOI	22.3	<0.001
μs	1.06	0.787

HbDiff: haemoglobin concentration difference; HbT: total haemoglobin concentration; LPR: lactate:pyruvate ratio; oxCCO: cytochrome c oxidation state; paO<sub>2</sub>: arterial pO<sub>2</sub>; pCO<sub>2</sub>: arterial pCO<sub>2</sub>; pbrO<sub>2</sub>: brain tissue pO<sub>2</sub>; TOI: tissue oxygenation index; SpO<sub>2</sub>: arterial oxygen saturation; μs: optical reduced scattering coefficient; Vmca: middle cerebral artery blood flow velocity.

was observed, post hoc testing identified no single epoch difference from baseline. Normobaric hyperoxia was also associated with statistically significant increases in Δ[oxCCO] and reductions in microdialysate LPR during the 0.6 FiO<sub>2</sub> (Δ[oxCCO]+0.18, *p*<0.01; ΔLPR −1.16, *p*<0.01) and 1.0 FiO<sub>2</sub> (Δ[oxCCO]+0.32, *p*<0.001; ΔLPR −3.07, *p*<0.01) epochs. These changes persisted in to the return-to-baseline epoch (Δ[oxCCO]+0.22 [*p*<0.01] and ΔLPR −0.254 [*p*<0.01]). Estimated CMRO<sub>2</sub> was higher in the return-to-baseline epoch compared to the baseline epoch [ΔCMRO<sub>2</sub> 107.5% of baseline (95% CI 100.3% – 119.0%, *p*=0.039)].

There were no changes in Δ[HbT] during the study. [HbDiff] increased during the 0.6 and 1.0 FiO<sub>2</sub> epochs (Δ[HbDiff]+1.18 μM and +2.17, respectively, both *p*<0.001), but there was no significant change during the return-to-baseline epoch compared to baseline. There was a significant increase in TOI during the 0.6 and 1.0 FiO<sub>2</sub> epochs (ΔTOI 2.8% and 6.0% respectively, both *p*<0.001), with no significant change during the return-to-baseline epoch. There were no significant changes in optical scattering measured at 790 nm (epoch effect *p*=0.786). There was no correlation between baseline pbrO<sub>2</sub> or LPR and the ΔLPR response to normobaric hyperoxia (*r*=−0.04, *p*=0.89; *r*=0.01 *p*=0.98, respectively).

## Discussion

We have demonstrated that normobaric hyperoxia-induced increase in pbrO<sub>2</sub> is associated with increased

[oxCCO] and reduced LPR, suggesting a change in mitochondrial redox status and the presence of oxygen dependent metabolism above traditionally described ischaemic thresholds. Our findings are consistent with oxygen-limited metabolism in this cohort of patients with acute brain injury, and suggest the presence of either oxygen diffusion limitation or mitochondrial dysfunction and hypoxia–ischaemia despite ‘normal’ values for pbrO<sub>2</sub>. Importantly, the [oxCCO] and LPR changes are sustained when FiO<sub>2</sub> is returned to baseline after the period of hyperoxia, while the markers of microvascular and brain tissue oxygenation (TOI, [HbO<sub>2</sub>], [HHb], pbrO<sub>2</sub>) return to their pre-hyperoxia values. This suggests that improvement in cellular metabolism persists beyond the immediate period of normobaric hyperoxia, a supposition supported by the elevation in estimated CMRO<sub>2</sub> during the return-to-baseline FiO<sub>2</sub> epoch.

Although the mean baseline pbrO<sub>2</sub> of 17.5 mmHg in our study lies within some definitions of hypoxia–ischaemia (<20 mmHg),<sup>36</sup> the majority of previous studies highlight <10 mmHg as a particular risk for elevated LPR and PET markers of ischaemia.<sup>37,38</sup> In our study, both epochs of the hyperoxia protocol resulted in elevation of pbrO<sub>2</sub> well into its ‘normal’ physiological range, and there was a stepwise increase in [oxCCO] and reduction in LPR as FiO<sub>2</sub> was increased from 0.6 to 1.0. These findings are not consistent with classical hypoxia–ischaemia. There was also no correlation between baseline pbrO<sub>2</sub> or LPR and the change in LPR, suggesting that hypoxia/ischaemia, defined by pbrO<sub>2</sub> or LPR, does not affect the brain’s response to normobaric hyperoxia in this patient group. This finding is unsurprising since the LPR was consistently reduced (−3.07 95% CI −4.38–1.61) during normobaric hyperoxia despite different baseline values for pbrO<sub>2</sub> and LPR.

Both oxygen diffusion abnormalities and mitochondrial dysfunction have been proposed as mechanisms for oxygen becoming a rate limiting substrate for metabolism.<sup>15,16,21</sup> Delivery of oxygen to the mitochondria is dependent on the gradient of oxygen tension as well as the conductance of the tissues. During the study period (24–72 h after ictus), cerebral oedema and hence perivascular/cellular swelling and microvascular collapse are important factors which increase the diffusion distance from the microvasculature to mitochondria and might necessitate increased oxygen tension to sustain the rate of mitochondrial oxygen delivery. However, our findings of sustained metabolic improvement ([oxCCO], LPR, CMRO<sub>2</sub>) on return-to-baseline FiO<sub>2</sub> and therefore baseline paO<sub>2</sub>, and predicted oxygenation gradients (see below), are not entirely consistent with diffusion limitation as the only pathological process. They may also indicate reversal

**Table 4.** Changes from baseline for measured variables data presented as (pseudo)median (95% confidence interval).

	Epoch		
	FiO <sub>2</sub> 0.6	FiO <sub>2</sub> 1.0	Return-to-baseline
Δ[HbDiff] (μM)	1.18 (0.59–2.12)	2.17 (1.17–4.13)	0.30 (–0.22–1.28)
Δ[HbT] (μM)	–0.13 (–0.52–0.22)	–0.46 (–1.16–0.13)	0.44 (–0.01–0.90)
Δ[oxCCO] (μM)	0.18 (0.08–0.47)	0.32 (0.11–0.76)	0.22 (0.06–0.62)
ΔTOI (%)	2.8 (1.8–5.6)	6.0 (3.4–10.9)	0.31 (–2.6–2.8)
Relative CMRO <sub>2</sub> (%)	–	–	107.5 (100.3–119.0)
Δ LPR	–1.16 (–1.93–0.455)	–3.07 (–4.38–1.61)	–2.54 (–4.38–0.475)
Δ pbrO <sub>2</sub> (mmHg)	8.44 (5.19–12.2)	30.9 (21.6–43.4)	2.72 (–1.76–9.46)
Δ MAP (mmHg)	1.19 (–2.32–4.92)	1.48 (–3.73–8.8)	–0.56 (–7.83–7.38)
Δ pCO <sub>2</sub> (kPa)	0.15 (0.0333–0.258)	0.114 (–0.05–0.258)	0.203 (–0.1–0.425)
Δ paO <sub>2</sub> (kPa)	14.1 (11.3–17)	38.7 (35–42.3)	–1.21 (–1.99–0.1)
Δ SpO <sub>2</sub> (%)	1.5 (1.00–2.00)	1.5 (1.01–2.00)	–0.831 (–1.16–0.778)
Vmca (cm.s <sup>–1</sup> )	2.19 (–1.23–5.62)	2.64 (–2.09–7.47)	5.19 (–0.45–11)
μs (cm <sup>–1</sup> )	0.0168 (–0.201–0.173)	–0.0201 (–0.394–0.297)	0.0785 (–0.423–0.354)

FiO<sub>2</sub>: inspired oxygen fraction; CMRO<sub>2</sub>: cerebral metabolic rate for oxygen; HbDiff: haemoglobin concentration difference; HbT: total haemoglobin concentration; LPR: lactate:pyruvate ratio; MAP: mean arterial blood pressure; oxCCO: cytochrome c oxidation state; paO<sub>2</sub>: arterial pO<sub>2</sub>; paCO<sub>2</sub>: arterial pCO<sub>2</sub>; pbrO<sub>2</sub>: brain tissue pO<sub>2</sub>; TOI: tissue oxygenation index; SpO<sub>2</sub>: arterial oxygen saturation; μs: optical reduced scattering coefficient; Vmca: middle cerebral artery blood flow velocity

of mitochondrial dysfunction by normobaric hyperoxia. Baseline TOI was 73% in our study and this lies within a physiologically ‘normal’ range for NIRS-derived regional cerebral saturation.<sup>39</sup> Assuming one-quarter of blood volume is saturated arterial blood, this predicts a venous saturation of 64% and approximate venous pO<sub>2</sub> of 33 mmHg (using the calculation from Menon et al.<sup>15</sup>), and thus an average difference of 15.5 mmHg between venous blood (33 mmHg) and pbrO<sub>2</sub> (17.5 mmHg). Similar comparisons using PET and pbrO<sub>2</sub> have described gradients of 10 mmHg and 27 mmHg in normal and impaired brain regions,<sup>15</sup> so our observations are consistent with only a moderate diffusion distance between the microvasculature and tissue interstitium. This further supports the notion that isolated diffusion limitation is not the sole mechanism implicated in oxygen becoming a rate limiting substrate for metabolism after acute brain injury.

CCO oxidation increased by 0.32 μM during a mean pbrO<sub>2</sub> change of 30.9 mmHg in the 1.0 FiO<sub>2</sub> epoch, and returned to 0.22 μM during return-to-baseline FiO<sub>2</sub>. Although the total concentration of CCO in the adult human brain is unknown, it is approximately 5 μM in rats.<sup>40</sup> The CCO changes that we observed are therefore likely to reflect an approximate 6% change in its oxidation, which is higher than that observed in healthy volunteers during increases in cerebral oxygen delivery or during functional activation,<sup>25,28,41,42</sup> but equivalent to those described previously in TBI.<sup>22</sup> The oxidation status of CCO is modified by both mitochondrial pO<sub>2</sub> and metabolic factors (ADP, NAD:NADH), and our findings are consistent with both an increase in aerobic metabolism and/or increased mitochondrial pO<sub>2</sub>. Earlier studies have shown an association between cerebral oxygen delivery and CCO oxidation in healthy volunteers<sup>25,43</sup> and, in animal models, with brain ATP<sup>40</sup>

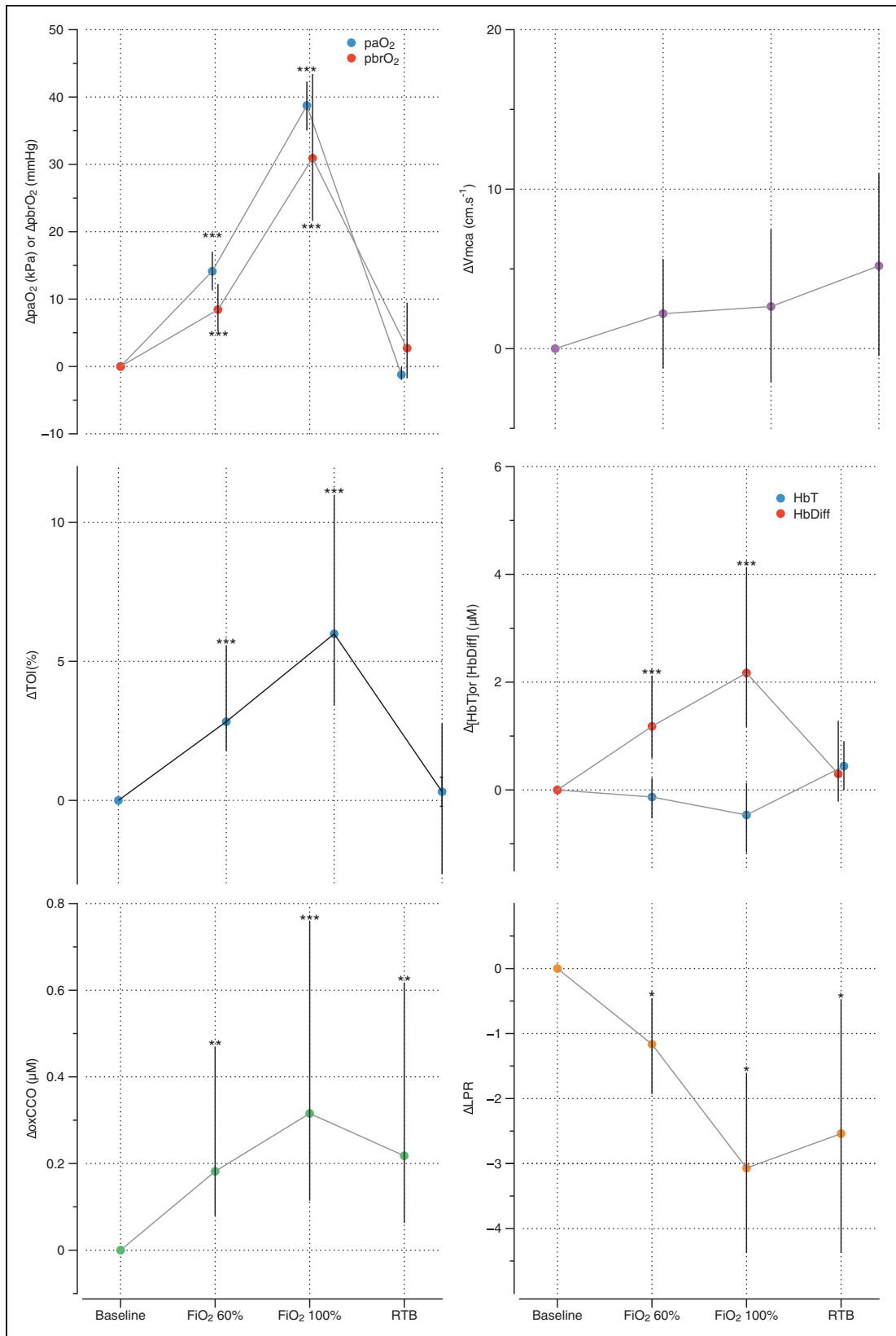


**Figure 2.** Changes in markers of cerebral oxygen delivery and aerobic metabolism during normobaric hyperoxia showing (pseudo)median changes and 95% confidence interval error bars.  
 \* $p < 0.05$ ; \*\* $p < 0.01$ ; \*\*\* $p < 0.001$ .

and lactate<sup>44</sup> concentrations. Likewise, the persistent CCO oxidation in the return-to-baseline epoch in our study suggests either increased aerobic metabolism (consistent with the measured LPR and estimated CMRO<sub>2</sub>) and/or an altered K<sub>m</sub> for O<sub>2</sub>. It is interesting to note that nitric oxide is known to increase the K<sub>m</sub> of CCO, and the proposed mechanism of action for normobaric and hyperbaric hyperoxia is the reversal of this nitric oxide effect thereby reducing the threshold at which oxygen becomes a rate limiting step in oxidative metabolism.<sup>24</sup> Thus, our results could theoretically represent the breakdown of NO rather than a direct effect of elevated mitochondrial pO<sub>2</sub>. Hypoxia-inducible factor 1 $\alpha$  (HIF-1 $\alpha$ ) is another major hypoxia signalling pathway which inhibits pyruvate dehydrogenase activity, a branch point controlling oxidative/anaerobic metabolism, as well as a range of glycolytic enzymes.<sup>45</sup> Although these effects may also be modified by hyperoxia, it has also been suggested that a reduction in LPR (as seen in our study) is more consistent with an increase in oxidative metabolism since HIF-1 $\alpha$  should reduce lactate while maintaining LPR.<sup>21</sup> While the median reduction in LPR (-3.07) during normobaric hyperoxia in our study is not large, and of unlikely clinical significance in itself, it might reflect a small volume of ischaemic tissue within the larger tissue volume monitored by the microdialysis catheter. Furthermore, when considered within the context of the increases in aerobic metabolism shown by the other monitoring modalities during normobaric hyperoxia, it is possible that this small improvement in LPR might indicate patients with an oxygen-dependent deficit in aerobic metabolism that is amenable to treatment. Further clinical studies are required to assess the clinical relevance of such changes in LPR when interpreted in association with other monitored variables of aerobic metabolism.

Our findings are consistent with those of several previous studies. Diringer et al. found no significant change in CMRO<sub>2</sub> in a PET study of normobaric hyperoxia in five TBI patients, but the small sample size precludes definitive conclusions. A pilot study by our group of eight patients with TBI found similar changes in LPR (-1.6) and  $\Delta$ [oxCCO] (+0.21  $\mu$ M) during normobaric hyperoxia to those we report here.<sup>22</sup> Our current study builds on that pilot in three important aspects – by including a larger number of patients, using an improved NIRS apparatus with patient-specific measures of differential pathlength factor, and incorporating an estimate of CMRO<sub>2</sub>. Nortje et al.<sup>21</sup> also demonstrated that normobaric hyperoxia in patients with TBI was associated with a similar reduction in LPR (mean LPR reduced from 34.1 to 32.5) to our current study, but PET-measured CMRO<sub>2</sub> increased only in regions of interest with a

reduced CMRO<sub>2</sub> at baseline. However, a smaller study of eight patients with TBI, showed no improvement in LPR during 3 h of normobaric hyperoxia.<sup>46</sup>

Our study demonstrated an improvement in markers of aerobic metabolism during a short (120 min) graded hyperoxia challenge. Although [oxCCO], LPR and CMRO<sub>2</sub> remained partially elevated following return-to-baseline FiO<sub>2</sub>, further assessments were not made beyond this period so the longevity of the potential metabolic benefit of hyperoxia is uncertain. It must be noted that hyperoxia has a variety of deleterious effects through generation of reactive oxygen species, induction of cytotoxic cytokines and immunosuppression, and concerns exist regarding its prolonged use. Kilgannon et al.<sup>47</sup> identified an association between supranormal paO<sub>2</sub> and worsened outcome following cardiac arrest, while Quintard et al.<sup>48</sup> demonstrated an association between normobaric hyperoxia and increased microdialysate glutamate, a key mediator of cerebral excitotoxicity, following TBI. While reactive oxygen species are a major injury mechanism implicated following cerebral ischaemia, they may be generated both by hypoxia (excess of reductive substrate) as well as by the delivery of excessive oxygen.<sup>49,50</sup> Thus, oxygen therapy must be carefully controlled after acute brain injury. Time-limited application of hyperoxia or the use of p<sub>br</sub>O<sub>2</sub> to guide oxygen administration may limit the potential deleterious effects of unrestrained oxygen use while minimising the risk of cerebral hypoxia/ischaemia. A higher p<sub>br</sub>O<sub>2</sub> might be warranted given the concerns with oxygen diffusion and mitochondrial inhibition 24–72 h post injury. Normobaric hyperoxia frequently results in restoration of p<sub>br</sub>O<sub>2</sub> into what is usually considered to be a ‘normoxic’ range, and the consistent increases observed in markers of aerobic metabolism even when p<sub>br</sub>O<sub>2</sub> is greater than the physiological range<sup>21–23</sup> might suggest the need for a higher target. Future research should focus on the relevance of higher p<sub>br</sub>O<sub>2</sub> targets and additional monitored variables that can inform oxygen therapy after acute brain injury.

Our study has several limitations. First, the individual monitoring modalities are designed to measure different aspects of the oxygen cascade and cellular bioenergetics, but each is subject to its own limitations. Although differential spectroscopy NIRS methodologies, such as the one we used to measure haemoglobin and [oxCCO] in this study, are subject to significantly more extracranial ‘contamination’ than spatially resolved spectroscopy techniques,<sup>39</sup> we have previously shown that [oxCCO] is a brain-specific signal with negligible contribution from extracranial tissues.<sup>25</sup> Furthermore, by measuring scattering and optical pathlength, we can place greater confidence on the accuracy of the measured change.<sup>40</sup> The differential spectroscopy



methodology that we used to measure changes in CCO oxidation is based on the modified Beer–Lambert law and therefore only able to quantify relative changes in chromophore concentration from an unknown baseline rather than measure absolute concentrations of oxidised and reduced CCO. Nevertheless, changes in CCO have been evaluated in animal models and shown to be a reliable measure of intracellular energy status.<sup>40,44,51</sup> Microdialysate LPR is an imperfect measure of cerebral aerobic metabolism. It reflects the activity of cytosolic lactate dehydrogenase, which is in large part reflective of intracellular NADH:NAD<sup>+</sup> ratio and thus related to the ability of mitochondria to produce ATP. There are therefore circumstances, including electron leak from the electron transport chain, during which LPR can be unchanged in the face of an inability of cells to generate energy.<sup>52</sup> Secondly, although we placed the microdialysis catheters in ‘at risk’ tissue in line with consensus guidelines,<sup>27</sup> used the same cranial access device for p<sub>br</sub>O<sub>2</sub> monitoring, and applied the NIRS optodes over the frontal region as close as possible to the insertion site of the invasive monitors, it is likely that different tissue volumes and regions were interrogated by each device. Similarly, it is difficult to know exactly what region of interest is represented by our estimate of CMRO<sub>2</sub> which is derived from Vmca (a relatively global measure of hemispheric CBF) and TOI (a regional measure of tissue oxygenation).<sup>39</sup> Finally, we investigated only 16 patients with mixed pathology, but this is a larger patient cohort than many investigations in this field – for example, those cited above – and the concept of an ischaemic p<sub>br</sub>O<sub>2</sub> threshold is relevant across all the pathologies included. Spatial heterogeneity is a limiting factor in the study of most acute brain injury types, and we have specifically targeted analysis of the injured hemisphere using a comprehensive array of monitoring modalities.

Overall, our findings highlight the difficulties in defining thresholds for hypoxia–ischaemia in the injured brain, and the potential risks to an individual of utilising generic targets to guide clinical management. Diffusion limitation and mitochondrial dysfunction may disrupt the normal relationship between OEF, p<sub>br</sub>O<sub>2</sub>, and mitochondrial redox status, and this might explain some observations of metabolic dysfunction ‘without hypoxia’ when either a diffusion barrier to oxygen is present (when p<sub>br</sub>O<sub>2</sub> and OEF may not reflect mitochondrial pO<sub>2</sub>) or much higher mitochondrial pO<sub>2</sub> is required to maintain ATP generation. Further studies employing multimodal monitoring, including [oxCCO], might shed further light on the exact nature of this metabolic derangement, and in the understanding of oxygen diffusion within the microvascular and intracellular environments, and oxygen utilisation. Extension of existing computational physiological models<sup>53</sup> may

assist in predicting oxygen diffusion gradients and utilisation, exploiting measurement of TOI, p<sub>br</sub>O<sub>2</sub> and CCO, and should be incorporated into future studies.

## Conclusion

Standard clinical therapy following acute brain injury fundamentally aims to avoid mitochondrial hypoxia in order to minimise secondary tissue ischaemia and worse clinical outcomes. p<sub>br</sub>O<sub>2</sub> and microdialysis-measured LPR have been used as surrogates of mitochondrial oxygen availability and its effect on mitochondrial redox status at the bedside, but clinical application and interpretation of such techniques requires clearly defined thresholds for ‘ischaemia’. Our results demonstrate an increase in oxCCO, reduction in LPR and increase in estimated CMRO<sub>2</sub> during and following normobaric hyperoxia. These findings are consistent with increased aerobic metabolism at p<sub>br</sub>O<sub>2</sub> levels higher than those typically recognised as ‘ischaemic’ thresholds. Such oxygen-limited metabolism suggests that hypoxia–ischaemia secondary to oxygen diffusion limitation or mitochondrial dysfunction might be prevalent after acute brain injury, and complicate assessment of ischaemia using measurement of p<sub>br</sub>O<sub>2</sub> in isolation. Simultaneous measurement of microvascular, tissue and cellular oxygenation and metabolism has potential to redefine our understanding of ischaemia after acute brain injury. Measurement of the oxidation status of CCO as a bedside, continuous assessment of mitochondrial energetics over multiple regions of interest has considerable potential to guide treatment after acute brain injury.

## Funding

The author(s) disclosed receipt of the following financial support for the research, authorship, and/or publication of this article: MS is supported in part by the Department of Health’s Institute for Health Research Centre’s funding scheme via the UCLH/UCL Biomedical Research Centre. AG was supported by a UK Medical Research Council Clinical Research Training Fellowship (G1000292). IT is supported by a Wellcome Trust senior fellowship (104580/Z/14/Z). This work was supported by the Engineering and Physical Sciences Research Council (EP/K020315/1) and Medical Research Council (17803).

## Declaration of conflicting interests

The author(s) declared no potential conflicts of interest with respect to the research, authorship, and/or publication of this article.

## Authors’ contributions

AG and DH are joint first authors and contributed equally. AG, IT, CEE, MS designed the study. AG performed the

research. AG, CK and DH analysed the data. AG, DH, IT, CEE, MS wrote the paper.

## References

- Kunz A, Dirnagl U and Mergenthaler P. Acute pathophysiological processes after ischaemic and traumatic brain injury. *Best Pract Res Clin Anaesthesiol* 2010; 24: 495–509.
- Cahill WJ, Calvert JH and Zhang JH. Mechanisms of early brain injury after subarachnoid hemorrhage. *J Cereb Blood Flow Metab* 2006; 26: 1341–1353.
- Qureshi AI, Mendelow AD and Hanley DF. Intracerebral haemorrhage. *Lancet* 2009; 373: 1632–1644.
- Loane DJ and Faden AI. Neuroprotection for traumatic brain injury: translational challenges and emerging therapeutic strategies. *Trends Pharmacol Sci* 2010; 31: 596–604.
- Tymianski M. Neuroprotective therapies: preclinical reproducibility is only part of the problem. *Sci Trans Med* 2015; 7: 299fs32.
- Connolly ES, Rabinstein AA, Carhuapoma JR, et al. Guidelines for the management of aneurysmal subarachnoid hemorrhage: a guideline for healthcare professionals from the American Heart Association/American Stroke Association. *Stroke* 2012; 43: 1711–1737.
- Brain Trauma Foundation, American Association of Neurological Surgeons, Congress of Neurological Surgeons. Guidelines for the management of severe traumatic brain injury. *J Neurotrauma* 2007; 24(Suppl 1): S1–S106.
- Vespa PM. Brain hypoxia and ischemia after traumatic brain injury. *JAMA Neurol* 2016; 73: 504.
- Veenith TV, Carter EL, Geeraerts T, et al. Pathophysiologic mechanisms of cerebral ischemia and diffusion hypoxia in traumatic brain injury. *JAMA Neurol* 2016; 73: 542–550.
- Krab K, Kempe H and Wikström M. Explaining the enigmatic KM for oxygen in cytochrome c oxidase: a kinetic model. *BBA – Bioenergetics* 2011; 1807: 348–358.
- Rolett EL, Azzawi A, Liu KJ, et al. Critical oxygen tension in rat brain: a combined (31)P-NMR and EPR oximetry study. *Am J Physiol Regul Integr Comp Physiol* 2000; 279: R9–R16.
- Scheffler K-M, Lehnert A, Rohrborn H-J, et al. Individual value of brain tissue oxygen pressure, microvascular oxygen saturation, cytochrome redox level, and energy metabolites in detecting critically reduced cerebral energy state during acute changes in global cerebral perfusion. *J Neurosurg Anesth* 2004; 16: 210–219.
- Ainslie PN, Shaw AD, Smith KJ, et al. Stability of cerebral metabolism and substrate availability in humans during hypoxia and hyperoxia. *Clin Sci* 2014; 126: 661–670.
- Coles JP, Fryer TD, Smielewski P, et al. Defining ischemic burden after traumatic brain injury using 15O PET imaging of cerebral physiology. *J Cereb Blood Flow Metab* 2004; 24: 191–201.
- Menon DK, Coles JP, Gupta AK, et al. Diffusion limited oxygen delivery following head injury. *Crit Care Med* 2004; 32: 1384–1390.
- Vespa P, Bergsneider M, Hattori N, et al. Metabolic crisis without brain ischemia is common after traumatic brain injury: a combined microdialysis and positron emission tomography study. *J Cereb Blood Flow Metab* 2005; 25: 763–774.
- Chen HI, Stiefel MF, Oddo M, et al. Detection of cerebral compromise with multimodality monitoring in patients with subarachnoid hemorrhage. *Neurosurgery* 2011; 69: 53–63; discussion 63.
- Vespa PM. Metabolic penumbra in intracerebral hemorrhage. *Stroke* 2009; 40: 1547–1548.
- Ko S-B, Choi HA, Parikh G, et al. Multimodality monitoring for cerebral perfusion pressure optimization in comatose patients with intracerebral hemorrhage. *Stroke* 2011; 42: 3087–3092.
- Geukens P and Oddo M. Brain tissue oxygen monitoring in neurocritical care. In: Vincent J-L (eds.) *Annual update in intensive care and emergency medicine 2012*. Berlin, Heidelberg: Springer, 2012, pp.735–745.
- Nortje J, Coles JP, Timofeev I, et al. Effect of hyperoxia on regional oxygenation and metabolism after severe traumatic brain injury: preliminary findings\*. *Crit Care Med* 2008; 36: 273–281.
- Tisdall MM, Tachtsidis I, Leung TS, et al. Increase in cerebral aerobic metabolism by normobaric hyperoxia after traumatic brain injury. *J Neurosurg* 2008; 109: 424–432.
- Kumaria A and Tolia CM. Normobaric hyperoxia therapy for traumatic brain injury and stroke: a review. *Br J Neurosurg* 2009; 23: 576–584.
- Cooper C. Competitive, reversible, physiological? Inhibition of mitochondrial cytochrome oxidase by nitric oxide. *IUBMB Life* 2003; 55: 591–597.
- Kolyva C, Ghosh A, Tachtsidis I, et al. Cytochrome c oxidase response to changes in cerebral oxygen delivery in the adult brain shows higher brain-specificity than haemoglobin. *Neuroimage* 2014; 85(Pt 1): 234–244.
- Roche-Labarbe N, Carp SA, Surova A, et al. Noninvasive optical measures of CBV, StO<sub>2</sub>, CBF index, and rCMRO<sub>2</sub> in human premature neonates' brains in the first six weeks of life. *Hum Brain Mapp* 2009; 31: 341–352.
- Hutchinson PJ, Jalloh I, Helmy A, et al. Consensus statement from the 2014 international microdialysis forum. *Intens Care Med* 2015; 41: 1517–1528.
- Kolyva C, Tachtsidis I, Ghosh A, et al. Systematic investigation of changes in oxidized cerebral cytochrome c oxidase concentration during frontal lobe activation in healthy adults. *Biomed Opt Exp* 2012; 3: 2550–2566.
- Matcher SJ, Elwell CE, Cooper CE, et al. Performance comparison of several published tissue near-infrared spectroscopy algorithms. *Analyt Biochem* 1995; 227: 54–68.
- Duncan A, Meek JH, Clemence M, et al. Optical path-length measurements on adult head, calf and forearm and the head of the newborn infant using phase resolved optical spectroscopy. *Phys Med Biol* 1995; 40: 295–304.

31. Suzuki S, Takasaki S, Ozaki T, et al. Tissue oxygenation monitor using NIR spatially resolved spectroscopy. *Proc SPIE* 1999; 3597: 582–592.
32. Roche-Labarbe NEG, Fenoglio A, Aggarwal A, et al. Near-infrared spectroscopy assessment of cerebral oxygen metabolism in the developing premature brain? *J Cerebr Blood F Metab* 2012; 32: 481–488.
33. Guo Y, Logan HL, Glueck DH, et al. Selecting a sample size for studies with repeated measures. *BMC Med Res Methodol* 2013; 13: 100.
34. R Core Team. *R: A language and environment for statistical computing*.
35. Laird NM and Ware JH. Random-effects models for longitudinal data. *Biometrics* 1982; 38: 963–974.
36. Longhi L, Pagan F, Valeriani V, et al. Monitoring brain tissue oxygen tension in brain-injured patients reveals hypoxic episodes in normal-appearing and in peri-focal tissue. *Intens Care Med* 2007; 33: 2136–2142.
37. Johnston AJ, Steiner LA, Coles JP, et al. Effect of cerebral perfusion pressure augmentation on regional oxygenation and metabolism after head injury\*. *Crit Care Med* 2005; 33: 189–195.
38. van den Brink WA, van Santbrink H, Steyerberg EW, et al. Brain oxygen tension in severe head injury. *Neurosurgery* 2000; 46: 868–878.
39. Ghosh A, Elwell C and Smith M. Review article: cerebral near-infrared spectroscopy in adults: a work in progress. *Anesth Analg* 2012; 115: 1373–1383.
40. Cooper CE and Springett R. Measurement of cytochrome oxidase and mitochondrial energetics by near-infrared spectroscopy. *Philos Trans R Soc Lond B Biol Sci* 1997; 352: 669–676.
41. Heekeren HR, Kohl M, Obrig H, et al. Noninvasive assessment of changes in cytochrome-c oxidase oxidation in human subjects during visual stimulation. *J Cerebr Blood Flow Metab* 1999; 19: 592–603.
42. Tachtsidis I, Tisdall MM, Leung TS, et al. Relationship between brain tissue haemodynamics, oxygenation and metabolism in the healthy human adult brain during hyperoxia and hypercapnea. *Adv Exp Med Biol* 2009; 645: 315–320.
43. Tisdall MM, Tachtsidis I, Leung TS, et al. Near-infrared spectroscopic quantification of changes in the concentration of oxidized cytochrome c oxidase in the healthy human brain during hypoxemia. *J Biomed Opt* 2007; 12: 024002.
44. Bainbridge A, Tachtsidis I, Faulkner SD, et al. Brain mitochondrial oxidative metabolism during and after cerebral hypoxia-ischemia studied by simultaneous phosphorus magnetic-resonance and broadband near-infrared spectroscopy. *Neuroimage* 2014; 102(Pt 1): 173–183.
45. Kietzmann T, Knabe W and Schmidt-Kastner R. Hypoxia and hypoxia-inducible factor modulated gene expression in brain: involvement in neuroprotection and cell death. *Eur Arch Psychiatr Clin Neurosci* 2001; 251: 170–178.
46. Magnoni S, Ghisoni L, Locatelli M, et al. Lack of improvement in cerebral metabolism after hyperoxia in severe head injury: a microdialysis study. *J Neurosurg* 2003; 98: 952–958.
47. Kilgannon JH, Kilgannon JH, Jones AE, et al. Relationship between supranormal oxygen tension and outcome after resuscitation from cardiac arrest. *Circulation* 2011; 123: 2717–2722.
48. Quintard H, Patet C, Suys T, et al. Normobaric hyperoxia is associated with increased cerebral excitotoxicity after severe traumatic brain injury. *Neurocrit Care* 2014; 22: 243–250.
49. Altemeier WA and Sinclair SE. Hyperoxia in the intensive care unit: why more is not always better. *Curr Opin Crit Care* 2007; 13: 73–78.
50. Guzy RD and Schumacker PT. Oxygen sensing by mitochondria at complex III: the paradox of increased reactive oxygen species during hypoxia. *Exp Physiol* 2006; 91: 807–819.
51. Cooper CE, Cope M, Springett R, et al. Use of mitochondrial inhibitors to demonstrate that cytochrome oxidase near-infrared spectroscopy can measure mitochondrial dysfunction noninvasively in the brain. *J Cerebr Blood Flow Metab* 1999; 19: 27–38.
52. Gjedde A, Gjedde A, Marrett S, et al. Glycolysis in neurons, not astrocytes, delays oxidative metabolism of human visual cortex during sustained checkerboard stimulation in vivo. *J Cerebr Blood Flow Metab* 2001; 21: 1384–1392.
53. Caldwell M, Hapuarachchi T, Highton D, et al. BrainSignals revisited: simplifying a computational model of cerebral physiology. *PLoS One* 2015; 10: e0126695.